Properties of 2D Bose gases at non-zero temperatures

Adrià Hernández Toledo

Supervisor: Pietro Massignan
Co-Supervisor: Andrea Richaud

Barcelona Quantum MonteCarlo group
08034 Barcelona

adria.hernandez.toledo@upc.edu

June 2025

In this work, we study the Berezinskii–Kosterlitz–Thouless (BKT) transition in two-dimensional ultracold Bose gases using the stochastic Gross–Pitaevskii equation at finite temperature. Through numerical simulations, we analyze several physical observables across the critical region, including the quasi-condensate density, vortex population, first-order correlation function $g^{(1)}(r)$, and superfluid density. Our results show clear signatures of the BKT transition: the onset of algebraic order in $g^{(1)}(r)$, the proliferation of free vortices above the critical temperature, and a universal jump in the superfluid density. We also examine the extent to which the energy distribution obeys the classical equipartition theorem. These findings demonstrate the effectiveness of stochastic Gross–Pitaevskii dynamics in capturing the essential features of 2D Bose gases across the BKT transition and provide insight into the interplay between coherence, topological defects, and superfluidity in low-dimensional systems.

Keywords: TFM, Quantum, Ultracold, Bose, Stochastic, BKT

Acknowledgements

I thank my supervisors, Pietro Massignan & Andrea Richaud, for their support and valuable insights throughout the development of this work. I also thank the Barcelona Quantum Montercarlo group at UPC for providing a favorable research environment.

Contents

1 Introduction

1.1 2D Bose Fluids

Back in 1925, Einstein predicted that, under a critical temperature T_c, in a gas of non-interacting bosons, a large portion would condense into the same quantum state. The regime for this phenomenon to be observed was at the time inaccessible, and the ideas of Einstein were neglected. Later, in 1937, Piotr Kapitsa and independently John F. Allen and Don Misener observed a remarkable property of helium II, the liquid phase of helium under 2.2 K : the ability to flow without viscosity. Its reminiscence with the behavior of superconductors, already discovered decades before, gained the phenomenon the name of *superfluidity*. These two, at the time unexplainable, phenomena, superconductivity and superfluidity, required the community for new ways of thinking. The ideas of Einstein were then recovered and several theories came forward. Today it is known that both superconductivity and superfluidity are manifestations of some degree of Bose-Einstein condensation. Einstein wrote about ideal gases, but these systems had far more intricate internal interactions. To observe what Einstein predicted, cooling techniques of gases needed to be refined. Finally, in 1995, the groups of Cornell and Wieman at JILA and Ketterle and MIT were able to observe the first gaseous Bose-Einstein condensate (BEC) in Rubidium atoms.

A phase transition is usually associated with a spontaneous breaking of a symmetry present in the Hamiltonian of the system. In a Bose-Einstein condensate, the order parameter encapsulating this information is the condensate density, which grows continuously below T_c. True long-range order is present and the phase of the wavefunction Ψ is randomly fixed, i.e., the condensate exists.

Dimensionality plays a central role in phase transitions and determines the types of order present in a physical system. Mermin, Wagner and Hohenberg rigorously proved [MW66] that it is impossible for systems with $d \leq 2$ to spontaneously break present symmetries at finite temperature. The existence of a Bose-Einstein condensate implies the spontaneous breaking of global U(1) phase symmetry. The global phase is randomly fixed and a true long-range order appears. In a uniform 2D system of bosons, thermal fluctuations are strong enough to destroy any fully ordered state, but not strong enough to suppress superfluidity.

In a 2D uniform boson system, a particular kind of transition takes place: The Berezinskii-Kosterlitz-Thouless (BKT) transition. The order of a phase transition is determined by the derivative of the free energy that suffers a discontinuity. The BKT transition is of infinite order, and links two unordered states. Under the critical temperature, there exists quasi-long-range order and superfluidity. Over the critical temperature, there is no long-range order and superfluidity is totally suppressed.

Although thermal fluctuations are enough to destroy long-range order, these scale smoothly with temperature and are not the source of the BKT transition. This transition is of topological nature, and can be explained by the presence of vortices. Vortices are points where the density vanishes and the phase around them varies by a multiple of $\pm 2\pi$. The circulation around these points is quantized, and the sign of the phase variation accounts for the sense of the rotation. Under the critical temperature $T_{\mathrm{BKT}}^{\infty}$, vortices only appear bound to antivortices. These pairs can alter the local phase around them, but having altogether a net circulation of zero, do not have long-range effects. In some sense, the creation of these pairs does not break the present topological order. Around the critical temperature, the system starts to favor the creation of free vortices and antivortices. When vortices and antivortices are free from each other, they cannot suppress each other's

phase fluctuations and completely scramble the phase of the system. By this mechanism, the topological order is destroyed and superfluidity vanishes.

1.2 Why 2D gases?

The study of two-dimensional physical systems has acquired a central role in contemporary physics, both experimentally and theoretically. 2D systems present unique collective behaviors in comparison with their 3D counterparts. As discussed above, 2D systems are very susceptible to thermal fluctuations to a point where the system is prevented from reaching a true long-range order, as established by the Mermin-Wagner-Hohenberg theorem [MW66].

Nevertheless, 2D gases present exclusive mechanisms of collective organization, based on topological properties instead of local symmetries. The paradigmatic example is the Berezinskii-Kosterlitz-Thouless (BKT) transition, which will be explored in detail in this work. This transition has been observed in a wide variety of systems [HD11], including superfluid and superconductor thin films, spin systems, and optically confined ultra-cold gases.

From an experimental point of view, the development of cooling techniques and confinement of atoms in optical traps has allowed the creation of highly controllable 2D systems in the laboratory setting. These platforms are used to simulate ideal Hamiltonians and observe directly the dynamics of the topological defects, spatial and temporal correlations, and the effects of dimensionality in the thermodynamics and out-of-equilibrium dynamics.

Two-dimensional systems not only presents a rich variety of phenomenology unique to their dimension, but also constitute a perfect laboratory to study topological transitions, correlation effects, and out-of-equilibrium quantum physics. Their study is essential, and thus extremely relevant, to further our understanding of fundamental aspects of quantum matter.

1.3 The Stochastic Projected Gross-Pitaevskii Equation

The time-dependent Gross-Pitaevskii equation (GPE) [Gro63] can successfully explain a wide range of the dynamics present in Bose-Einstein condensates at zero temperature. First introduced in 1962 [Gro63], this mean-field approximation describes a dilute, weakly interacting gas of bosons that can be represented by a single wavefunction Ψ. The equation, reminiscent of a Schrödinger equation, evolves the wavefunction Ψ while ignoring all incoherent processes. Although this is not an issue at zero temperature, at finite temperatures experiments have produced results inconsistent with the GPE [AZBP13, GRM14].

Great efforts have been made in the last years to develop kinetic theories [PRS24] that encapsulate coherent and incoherent processes in a tractable manner. At zero temperature, an almost perfect condensate forms, meaning that a macroscopic fraction of the atoms is in the ground state. When the temperature starts to rise, higher modes will start to be sparsely occupied. In order to account for the new occupied modes and their effect on the properties of the gas, i.e., to have a successful description, we split the modes into 2 regions:

- **C-field region:** Contains the ground state and all the other highly degenerate modes. It can also contain modes of low occupation that are relevant for the dynamics of the system. This region is therefore the one that we aim to successfully represent.

- **Incoherent region:** The remaining modes, which are assumed to have almost no influence in the dynamics of the c-field region. Although these modes' static and

dynamical properties are not necessarily incoherent by nature, they can be very well approximated as being incoherent.

Kinetic theories aim at incorporating both regions have led to a modified Gross-Pitaevskii equation, which will be the core of this project.

To restrict the evolution strictly to the C-field, the first modification is to apply a projection operator. The C-field region becomes a microcanonical system, isolated from the incoherent region, matching its chemical potential and temperature. The projection operator can be easily applied in the momentum space, as it will be discussed in 1.4. To correctly isolate the incoherent region, a proper cut-off energy has to be chosen. This energy will define the maximum momentum on the projection: $\varepsilon_{cut} = \frac{\hbar^2 k_{cut}^2}{2m}$. A good criterion for this energy cut-off is to inspect the Bose-Einstein distribution for mean occupations as low as 1. This then yields $\varepsilon_{max} = \mu + k_B T \ln 2$. This sole modification is known as the Projected Gross-Pitaevskii equation (PGPE).

For some cases, the coupling between the C-region and the incoherent region cannot be neglected. Under this premise, the C-region can now exchange particles and energy with the incoherent region, i.e, behaves as a grand canonical system. Different derivations [PRS24, GD03, BBD+08] were developed from first principles, converging to the same equation in the regime we are interested in this work (weakly-interacting gases interacting via contact potential). The Stochastic Projected Gross-Pitaevskii equation modifies the PGPE by adding a noise term η that accommodates thermal fluctuations and a damping γ that allows the dissipation of energy due to the interaction with the incoherent region, fulfilling the fluctuation-dissipation theorem [PRS24]. Different forms of the equation can be found in scientific publications these recent years [CLDP19, KC16], but the one used in this project is:

$$i\hbar\frac{\partial\Psi}{\partial t} = \mathcal{P}\left\{(1-i\gamma)\left[-\frac{\hbar^2}{2m}\nabla^2 + V + g|\Psi|^2\right]\Psi + \eta\right\}. \tag{1}$$

The two main modifications with respect to the regular GPE are:

- The projector $\mathcal{P} = \Theta\left(\varepsilon_{cut} - \varepsilon\right)$, introduced on the PGPE. In the momenta space takes the form $\mathcal{P} = \sum_{\mathbf{k}=0}^{\mathbf{k}=\mathbf{k_{cut}}} |\psi_{\mathbf{k}}\rangle \langle\psi_{\mathbf{k}}|$.
- Thermal fluctuations η and the effective dissipation rate or damping γ. The correlation function of the noise, or variance, derived from the dissipation-fluctuation theorem, is $\langle\eta(\mathbf{r},t)\eta(\mathbf{r}',t')\rangle = 2\hbar\gamma k_B T\delta(t-t')\delta(\mathbf{r}-\mathbf{r}')$. The effective dissipation rate γ is considered a constant in the regime of this work and regulates the coupling between the regions.

The original developments of the SPGPE allowed for exchange of particles between coherent and incoherent regions. This translates to a non-fixed norm when solving the equation numerically. The fact that our system has an analytical solution for the number of incoherent density [CGIA24], $n_{incoh} = \int \frac{d\mathbf{k}}{(2\pi)^d} \frac{\Theta(|\mathbf{k}|-k_{cut})}{e^{\hbar^2\mathbf{k}^2/2mk_BT}-1} = \frac{k_B T m \log 2}{2\pi\hbar^2}$, made us consider a norm-fixed solution, which, in principle, is easier to solve numerically. For the grand canonical case, the chemical potential μ is introduced in the Hamiltonian and needs to be determined implicitly by evolving the equation for different μ and extrapolate the value for which the system equilibrates at the desired density. In this work, we have addopted a different approach: the norm is fixed at the number of coherent particles $N_{coh} = L_x L_y n_{coh}$, which is computed as $n_{coh} = n_0 - n_{incoh}$, and introduce a chemical potential $\mu_0 = n_{coh} g$. The reduction from the grand canonical to the canonical ensemble is justified if the system is large enough: once the chemical potential is fixed, the central limit theorem entails only very small fluctuations of the norm.

1.4 Implementation

All the results presented in this work were obtained by numerically solving the SPGPE with a pseudo-spectral first-order Euler scheme (see Appendix A.0.1) using the Numpy library.

Let us describe an iteration of the procedure; the aim of each iteration is to calculate

$$\Psi_{j+1} = \Psi_j + \left\{ \frac{-idt}{\hbar}(1 - i\gamma) \left[-\frac{\hbar^2}{2m}\nabla^2 + V + g|\Psi_j|^2 \right] \Psi_j + \eta_j \right\},$$

and project the wavefunction Ψ_{j+1} onto the corresponding subspace.

- The Laplacian of Ψ is calculated in the momentum space, $\nabla^2\Psi_j = \mathrm{IFFT}\{-(k_x^2 + k_y^2)\mathrm{FFT}\{\Psi_j\}\}$. The adoption of a Fast-Fourier-Transform-based approach automatically imposes periodic boundary conditions , which well represent a uniform system like the one simulated.

- The noise η is computed directly from its correlation function. To ensure temporal independence, it is regenerated in each iteration and, at each point in space, takes the form $\eta = \sqrt{\frac{\hbar\gamma k_B T}{dx\, dy\, dt}}(\mathrm{N}(0,1) + i\mathrm{N}(0,1))$, where $\mathrm{N}(0,1)$ is a number extracted from a gaussian distribution of mean 0 and standard deviation 1.

Then, the projector $\mathcal{P}$ is applied as a Boolean mask, cutting off the modes with a momentum above $k_{cut} = \frac{\sqrt{2m\varepsilon_{cut}}}{\hbar}$.

The system eventually reaches equilibrium after a number of iterations. Given the stochastic nature of the equation, every quantity of interest extracted from the wavefunction Ψ needs to be averaged over many times, sampled after the thermal equilibrium is reached. In some cases, these quantities can also be averaged over different evolutions to enforce the generation of random numbers.

To correctly track the convergence of the system, we decided to follow the evolution of the energy,

$$E = \int d^2\mathbf{r} \left[\frac{\hbar^2}{2m}|\nabla\Psi(\vec{r},t)|^2 + \frac{g}{2}|\Psi(\vec{r},t)|^4 \right]. \tag{2}$$

The system is free of external interactions and the Hamiltonian is constant in time, but noise and damping are present, thus after some transient time the energy fluctuates around some stable value, as shown for a typical simulation in Fig. 1.

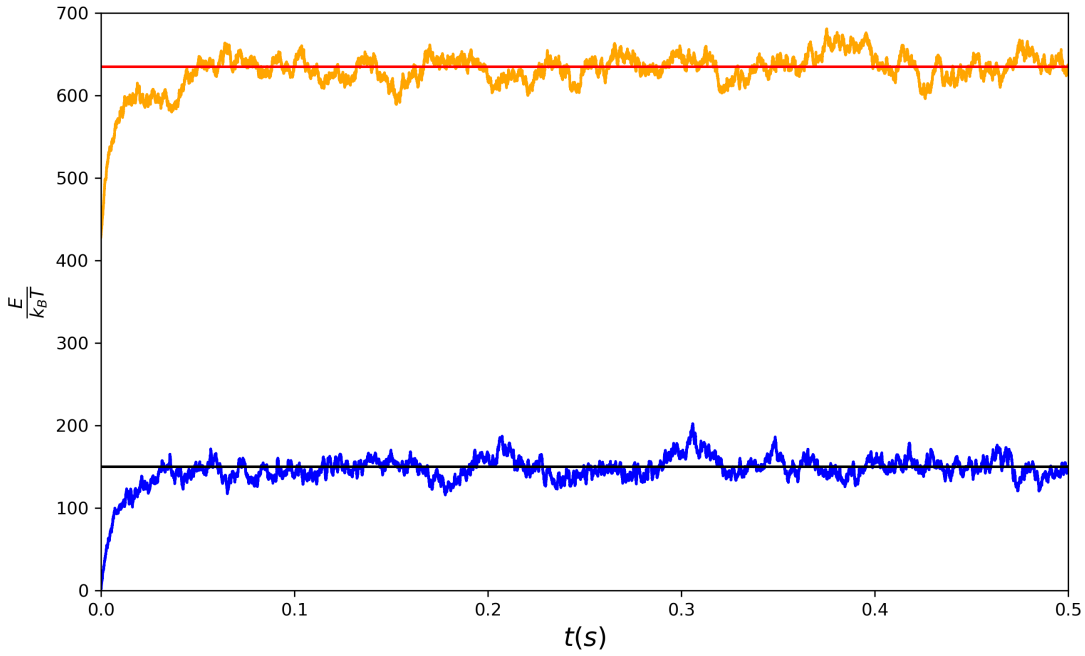

Figure 1: Total energy (in orange) and kinetic energy (in blue) with their values at convergence (horizontal lines.)

The system parameters used in this project have already been used in [CLDP19] and [CGIA24] and link to the parameters used to model quasi-2D gases in a series of experiments with ^{87}Rb at Laboratoire Kastler Brossel [CCB+15, VSL+18, SJCC+19].

Such parameters are: a mass $m = 1.4431 \cdot 10^{-25}$ kg, average density $n_0 = 9\ \mu\text{m}^{-2}$ and interaction strength $g = 7.32 \cdot 10^{-45}\ \text{J} \cdot \text{m}^2$. For a weakly-interacting gas with this system parameters, the critical temperature is [PS02]:

$$T_{\text{BKT}}^{\infty} = \frac{\hbar^2 2\pi n_0}{k_B m \log(380\hbar^2/mg)} = 38.05\text{nK} \tag{3}$$

This expression is derived combining the predictions of the BKT theory and Montecarlo simulations.

The structure of this work is as follows: Sec. 2 presents the results for the quasicondensate fraction n_{qc} and the vortex density n_V (see 2.1), the first order correlation function $g^{(1)}(r)$ (see 2.2), the superfluid fraction f_s (see 2.3) and a discussion on the Equipartition theorem (see 2.4). Sec. 3 provides the conclusions and possible directions for future research. The Appendix A contains relevant code used in the simulations.

2 Results

2.1 Quasicondensate fraction and vortex formation

As discussed above, a 2D Bose gas with interactions cannot exhibit true long-range order at finite temperature [HD11], i.e., it cannot form a true condensate. The quasi-long-range coherence present in the gas leads to the formation of a quasicondensate, which can be understood as a condensate with a fluctuating phase. The quasicondensate fraction [PRS01] is defined as

$$n_{qc} = \frac{\sqrt{2\langle\langle|\Psi(\vec{r},t)|^2\rangle\rangle^2 - \langle\langle|\Psi(\vec{r},t)|^4\rangle\rangle}}{\langle\langle|\Psi(\vec{r},t)|^2\rangle\rangle}. \tag{4}$$

This quantity is local and does not present finite size effects. It is a quantifier of the local order in the gas. Given that the SPGPE is of stochastic nature, the averages need to be performed also over stochastic realizations. The double brackets $\langle\langle ... \rangle\rangle$ indicate averages over the grid and also over equilibrated realizations of the field $\Psi(\vec{r},t)$.

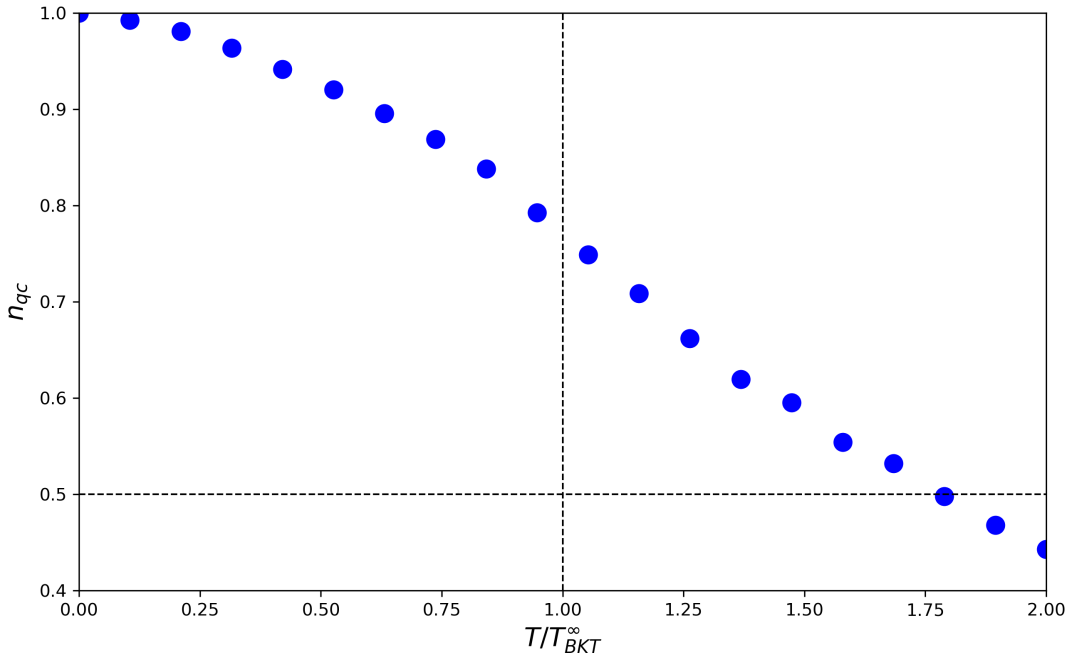

Figure 2: Quasicondensate fraction n_{qc} as a function of the system's temperature.

As presented in Fig. 2., the quasicondensate has a non-zero value at the critical temperature ($n_{qc} \approx 0.75$) and decreases steadily in the range of study.

Vortices are the central phenomenon that explain the BKT transition. The fact that above a critical temperature they proliferate and no longer form bound dipoles destroys the coherence in the gas and suppresses superfluidity. This will be discussed in more detail in Section 2.3. To calculate the number of vortices, I programmed a function (see Appendix A.0.2) to count vortices inspired by the library *VortexDistributions.jl* [Bra24], which calculates the phase difference between the 4 nearest points of the point of interest to detect if there is a vortex or antivortex. The proliferation of vortices creates local phase fluctuations. If these vortices are free, these fluctuations have a long-range effect and disrupt the domains of coherence present in the gas, suppressing superfluidity.

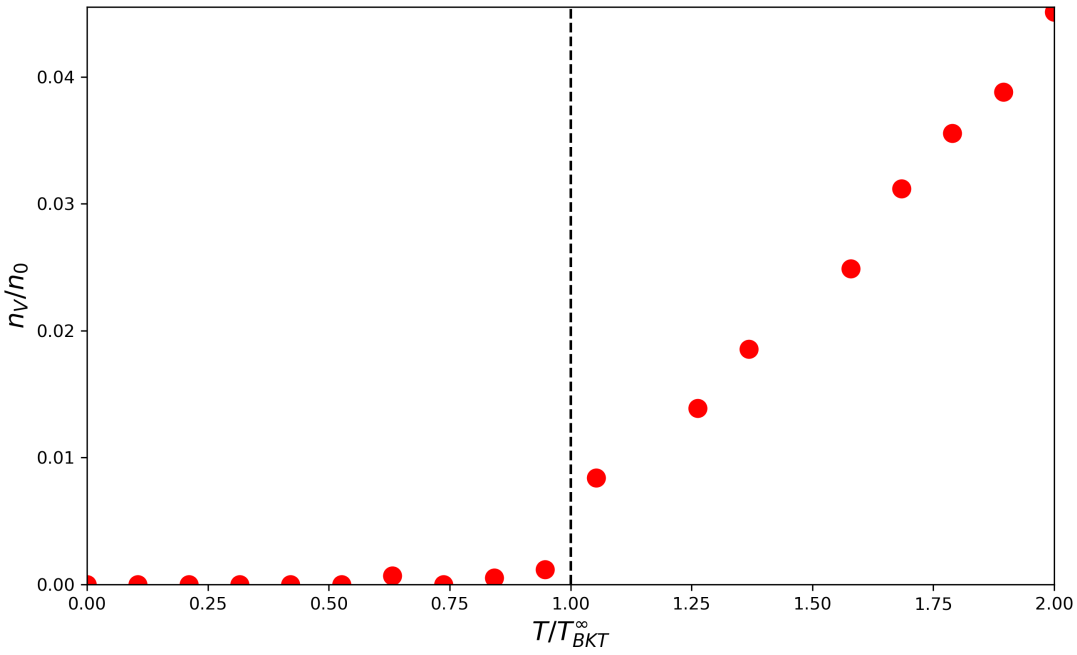

Figure 3: Density of vortices, defined as the number of vortices per unit area normalized to the number density n_0, as a function of the system's temperature.

Each vortex is bound to an antivortex below $T^{\infty}_{\mathrm{BKT}}$. Near the critical temperature, free vortices start to develop and their number grows rapidly. To better visualize this phenomenon, 3 snapshots of each regime are presented.

2.1.1 Low-temperature regime

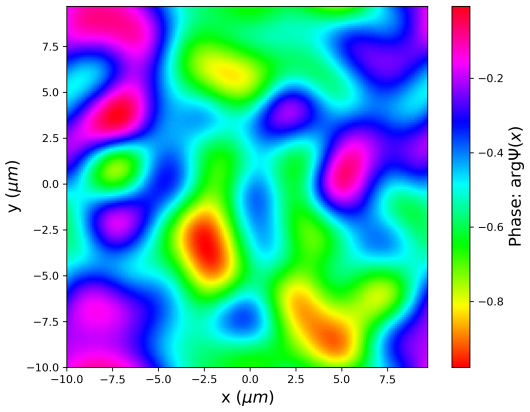

Figure 4: Phase snapshot of an equilibrium state at $T = 0.1T^{\infty}_{\mathrm{BKT}}$

The low-temperature regime is the one of temperatures well below $T^{\infty}_{\mathrm{BKT}}$.
In this regime, big domains of phase coherence are present, as seen in Fig. 4. The variability of phase is small, and no sudden change of phase is observed, which would be an indicator of vortex presence.

2.1.2 Transition regime

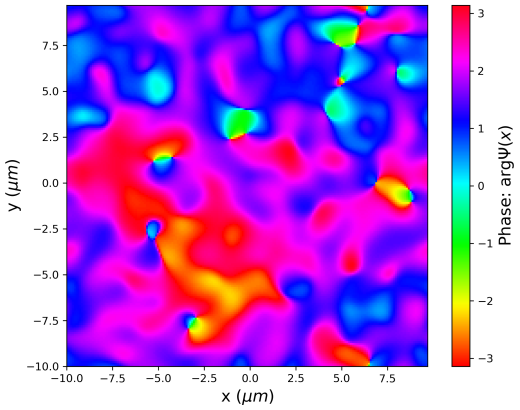

The transition regime corresponds to the temperature around the transition temperature $T^{\infty}_{\mathrm{BKT}}$.
The domains of phase coherence are smaller than in the previous case. In Fig. 5 we can observe the full range of phases $[-\pi, \pi]$, with some sudden changes of phase between neighbor points, indicating the presence of a reduced number vortices.

Figure 5: Phase snapshot of an equilibrium state at $T = 0.9T^{\infty}_{\mathrm{BKT}}$

2.1.3 Thermal regime

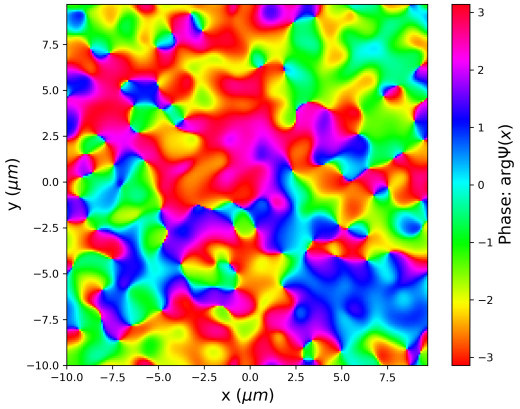

The thermal regime corresponds to temperatures well above the the transition temperature $T^{\infty}_{\mathrm{BKT}}$.
As seen in Fig. 6, phases are all scrambled up, and considerable number of sudden changes of phase between near points is observed, indicating the presence of vortices.

Figure 6: Phase snapshot of an equilibrium state at $T = 1.5T^{\infty}_{\mathrm{BKT}}$

The 3 presented snapshots are concrete cases of what is shown in Fig. 2 and in Fig. 3.

2.2 First order correlation function $g^{(1)}(r)$

The first order correlation function $g^{(1)}(r)$ is a quantifier of the coherence present in the system. As opposed to the quasicondensate fraction n_{qc}, $g^{(1)}(r)$ is a global quantity, presents finite size effects, and quantifies the phase fluctuations. It also shows the lack of true condensation in the 2D weakly-interacting uniform Bose gas: following the definition of the condensate density n_c given by Penrose & Onsager [PO56]

$$n_c = \lim_{r \to \infty} g^{(1)}(r), \tag{5}$$

$g^{(1)}(r)$ always tends to 0 at $r \to \infty$, indicating no condensate formation.

For the field $\Psi(\vec{r},t)$,

$$g^{(1)}(r) = \frac{\langle \Psi^*(\vec{r}_0)\Psi(\vec{r}_0+\vec{r})\rangle_{\vec{r}_0,\theta,\mathcal{M}}}{\sqrt{\langle|\Psi^*(\vec{r}_0)|^2\rangle_{\vec{r}_0,\theta,\mathcal{M}}\langle|\Psi(\vec{r}_0+\vec{r})|^2\rangle_{\vec{r}_0,\theta,\mathcal{M}}}} \tag{6}$$

where the averages are over the spatial point $\vec{r}_0$, the angular part θ and $\mathcal{M}$ stochastic realizations. The calculation of $g^{(1)}(r)$ through this expression is computationally demanding. A more convenient way to obtain it is through the Wiener-Khinchin theorem (see Appendix A.0.3), used in previous works for the same aim [CGIA24]. The theorem simplifies the calculation of the numerator, where the relevant information lies, through Fourier transformations.

$$\langle \Psi^*(\vec{r}_0)\Psi(\vec{r}_0+\vec{r})\rangle_{\vec{r}_0,\theta,\mathcal{M}} = \mathrm{IFFT}\left\{|\mathrm{FFT}\{\Psi(\vec{r})\}|^2\right\}. \tag{7}$$

The theoretical framework [KT73] predicts two well differentiated behaviors of $g^{(1)}(r)$:

- For $T < T^{\infty}_{\mathrm{BKT}}$, an algebraic decay is expected, $g^{(1)}(r) \sim r^{-\alpha}$.
- For $T > T^{\infty}_{\mathrm{BKT}}$, an exponential decay is expected, $g^{(1)}(r) \sim e^{-r/\xi}$, where ξ is the healing length $\xi = \hbar/\sqrt{2mgn_0}$.

The theoretical framework [KT73] of the BKT transition also predicts the value of the exponent α at the transition, $\alpha_c = 0.25$. Let us inspect how the SPGPE successfully reproduces the theoretical predictions.

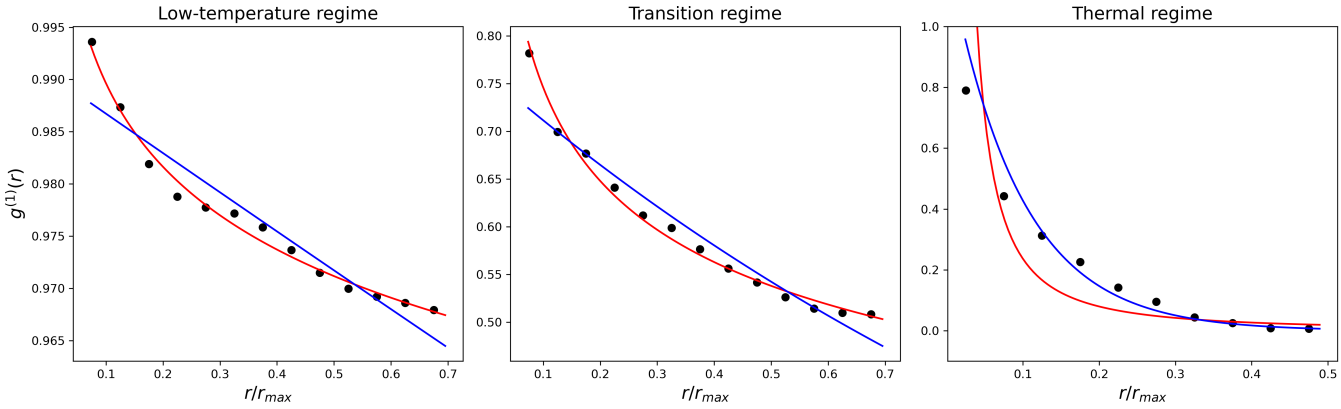

Figure 7: $g^{(1)}(r)$ (black dots) and algebraic (red lines) and exponential (blue lines) fits for 3 temperatures. From left to right: $0.1T^{\infty}_{\mathrm{BKT}}$, $0.9T^{\infty}_{\mathrm{BKT}}$ and $1.5T^{\infty}_{\mathrm{BKT}}$

For temperatures below the transition, free vortices do not proliferate. Thus, a slow decay in $g^{(1)}(r)$ is expected, which is a quantifier of the coherence in the system. Fig. 7 (a) and Fig. 7 (b) show that an algebraic fit adjusts with high precision to the data extracted from the SPGPE. The α's extracted from the fits are, respectively, 0.012 and 0.20. For temperatures above the transition, free vortices proliferate, scrambling the phases and destroying any semblance of coherence. Thus, a much faster decaying $g^{(1)}(r)$ is expected. Fig. 7 (c) shows how the algebraic fit is less accurate than in the previous cases, while the exponential fit matches the data with higher precision.

The data match the expected behavior of the fitted curves, but it is left to determine if, for the algebraic cases, the exponent is correctly reproduced. Although the theory only predicts the value of the exponent α at $T^{\infty}_{\mathrm{BKT}}$, from Fig. 7 a prediction of its evolution with

temperature can be conjectured. For $T < T^{\infty}_{\mathrm{BKT}}$, the exponent α should increase steadily, and for $T > T^{\infty}_{\mathrm{BKT}}$ it should increase faster until it diverges.

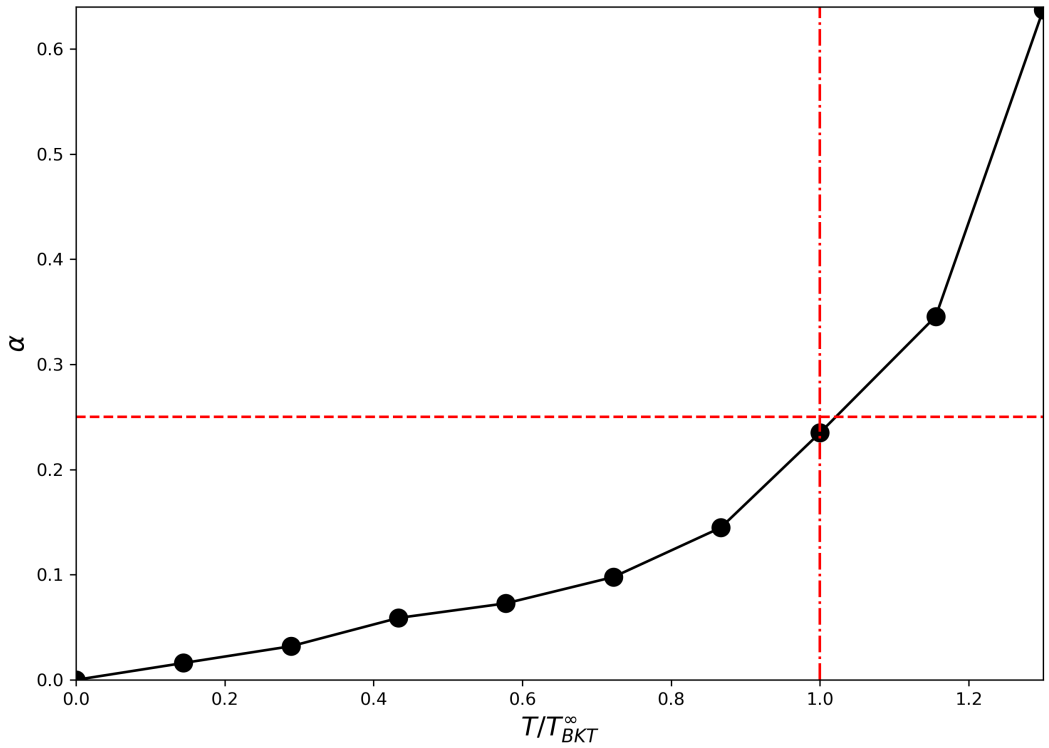

Figure 8: Evolution of the exponent α with temperature.

The model effectively reproduces the value of the exponent α at the transition. The value obtained and presented in Fig. 8 is $\alpha_c = 0.235$. It is important to note that a uniform system of fixed sized is being simulated. The BKT predictions are made in the thermodynamic limit, i.e., an infinite system. For the exact 0.25 value, the system size and particle number should tend to ∞ while maintaining a constant density.

2.3 Superfluid fraction

Although superfluidity is often linked to Bose-Einstein condensation, systems with no true long-range order, such as the uniform Bose gas studied, can be superfluid. The BKT transition, as discussed above, is a topological transition between a quasi-long-range order state with bound pairs of vortex-antivortex to a disordered state with freely distributed vortices. It can also be seen as a transition between a partially superfluid state and a completely normal, in the classical sense, fluid state. The BKT framework predicts a total vanishing of superfluidity at the transition. In a quantum fluid, one can differentiate between the *superfluid fraction* f_s and the *normal fraction* $f_n = 1 - f_s$. The normal fraction is the part of the system that behaves classically, and the superfluid fraction is the part of the system that presents quantum properties. One of these properties is the absence of viscosity. If the gas is at rest in a tube, and the tube is set in motion at a low velocity with respect to the laboratory frame reference, the superfluid component will remain at rest,

while the normal component of the gas will be dragged with the walls of the tube. This idea, as presented in [Dal24], can be applied to our equation to compute the superfluid fraction $f_s = \frac{\rho_s}{\rho}$. Let us describe the procedure:

1. A perturbation $-\hat{P}\cdot\vec{v}$ is added to the SPGPE. This perturbation formally corresponds to a change of reference frame to a one moving with velocity $\vec{v}$ with respect to the laboratory reference frame. The momentum operator $\hat{P}$ is the total momentum of the gas particles in the laboratory reference frame.

$$i\hbar\frac{\partial\Psi}{\partial t} = \mathcal{P}\left\{(1-i\gamma)\left[-\frac{\hbar^2}{2m}\nabla^2 + V + g|\Psi|^2 - \hat{P}\cdot\vec{v}\right]\Psi + \eta\right\}. \tag{8}$$

   In our implementation, the perturbation only affects the x axis. The total momentum operator $\hat{P}$ is calculated as $\hbar k_x$ in Fourier space, and the velocity is chosen as a fraction of the sound speed in the gas, $v_x = 0.3\sqrt{\frac{gn_{coh}}{m}}$. It is mandatory to use a low velocity to stay in the linear response regime. The equation with the perturbation evolves $\Psi(\vec{r},t)$ until it reaches equilibrium.

2. The gas at rest has an average momentum $\langle\hat{P}\rangle_{v_x=0} = 0$. When the perturbation is added, and as discussed above, only the normal component of the gas will be affected. Thus, the average momentum of the system will inform about the number of particles behaving classically: $\langle\hat{P}\rangle_{v_x} = f_n N_{coh} m v_x$. By calculating the average momentum, the normal fraction f_n is determined, and thus the superfluid fraction f_s:

$$f_s = 1 - \frac{\langle\hat{P}\rangle_{v_x}}{N_{coh} m v_x}. \tag{9}$$

   As for previous quantities of interest, f_s is averaged over a large number of iterations.

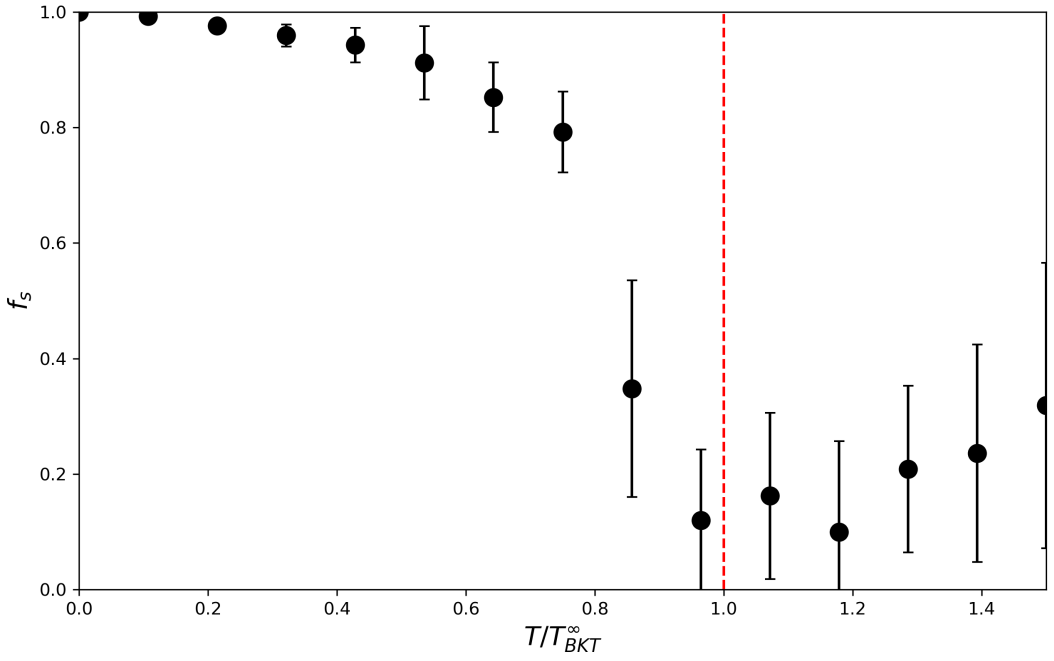

Figure 9: Superfluid fraction f_s as a function of the system's temperature.

The BKT framework predicts a sharp jump to zero at transition in the thermodynamic limit. Previous works on this subject [PS02, GB19] have reported the difficulty of observing this phenomenon in a finite size system like the one it is being simulated. In Fig. 9, the signature of the jump can be observed near $T^{\infty}_{\mathrm{BKT}}$. The data points above the transition are non-zero. After several numerical tests, we believe it to be a limitation of the model as opposed to numerical errors. The error bars are included to show that the results are compatible with the theoretical framework.

2.4 Equipartition theorem

The equipartition theorem [Pat96], a central result in classical statistical mechanics, states that

$$\left\langle q_m \frac{\partial H}{\partial q_n} \right\rangle = \delta_{mn} k_B T, \tag{10}$$

where q_n and q_m are degrees of freedom of the system and H the Hamiltonian of the system.

Although a Bose gas is essentially a quantum system, the mean-field treatment of the GPE encapsulates the system information in a macroscopic wavefunction $\Psi(\vec{r}, t)$, which is mathematically analogue to a classical field. In addition, the stochastic component added in agreement with the Fluctuation-Dissipation theorem [PRS24] ensures that the system reaches the thermal equilibrium. The conditions needed for the application of the equipartition theorem are then met.

For the classical field $\Psi(\vec{r}, t)$ involved in the SPGPE, the Hamiltonian of the system is:

$$H[\Psi] = \int d^2\mathbf{r} \left[\frac{\hbar^2}{2m} |\nabla \Psi(\vec{r}, t)|^2 + \frac{g}{2} |\Psi(\vec{r}, t)|^4 \right]. \tag{11}$$

Restricting to the kinetic term, which is a valid assumption for $T \gg T^{\infty}_{\mathrm{BKT}}$, and switching to momentum space $\Psi(\vec{r}, t) = \sum_{\vec{k}} \Psi_{\vec{k}} \mathrm{e}^{i\vec{r}\cdot\vec{k}}$, the Hamiltonian takes the form

$$H_{kin}[\Psi] = \int d^2\mathbf{r} \left[\frac{\hbar^2}{2m} |\nabla \Psi(\vec{r}, t)|^2 \right] = \sum_{\vec{k}} \frac{\hbar^2 k^2}{2m} |\Psi_{\vec{k}}|^2. \tag{12}$$

In this formalism, $\Psi_{\vec{k}}$ is a complex function, and, as such, admits the decomposition $\Psi_{\vec{k}} = a_{\vec{k}} + i b_{\vec{k}}$. Rewriting the Hamiltonian in this form allows for the application of the theorem.

$$H_{kin}[\Psi_{\vec{k}}] = \sum_{\vec{k}} \frac{\hbar^2 k^2}{2m} (a^2_{\vec{k}} + b^2_{\vec{k}}), \tag{13}$$

$$E^{eq}_{kin} = \left\langle H_{kin}[\Psi_{\vec{k}}] \right\rangle = \sum_{\vec{k}} \frac{\hbar^2 k^2}{2m} \langle a^2_{\vec{k}} \rangle + \sum_{\vec{k}} \frac{\hbar^2 k^2}{2m} \langle b^2_{\vec{k}} \rangle \tag{14}$$

$$= \sum_{\vec{k}} \frac{1}{2} \left\langle a_{\vec{k}} \frac{\partial H_{kin}}{\partial a_{\vec{k}}} \right\rangle + \sum_{\vec{k}} \frac{1}{2} \left\langle b_{\vec{k}} \frac{\partial H_{kin}}{\partial b_{\vec{k}}} \right\rangle \tag{15}$$

$$= \sum_{\vec{k}} \left(\frac{1}{2} k_B T + \frac{1}{2} k_B T \right) \tag{16}$$

$$= N_{\vec{k}} k_B T \tag{17}$$

where $N_{\vec{k}}$ is the number of modes in the momentum space. For a system of box size L^d and dimension d:

$$N_{\vec{k}} = \left(\frac{L}{2\pi}\right)^d \int_{|\vec{k}|\leq k_{cut}} d^d\mathbf{k} \propto k_{cut}^d, \tag{18}$$

and, as $k_{cut} \propto T^{1/2}$ for $T \gg T_{\mathrm{BKT}}^{\infty}$,

$$E_{kin}^{eq} \propto T^{d/2+1}. \tag{19}$$

Then, for 2D:

$$N_{\vec{k}}^{2D} = \frac{L^2 k_{cut}^2}{4\pi}, \tag{20}$$

and,

$$E_{kin}^{eq,\ 2D} = \frac{L^2 k_{cut}^2}{4\pi} k_B T \propto T^2. \tag{21}$$

In our implementation, $N_{\vec{k}}^{2D}$ can be calculated as the points of the FFT grid inside the masked momentum space.

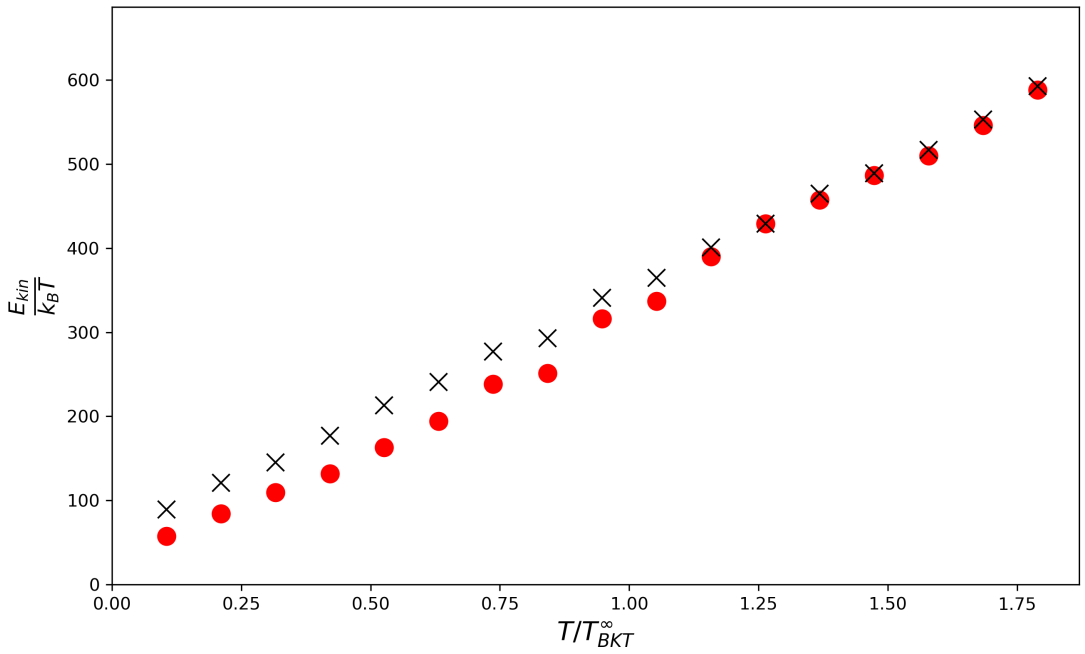

Figure 10: Kinetic energy numerically calculated (red dots), and kinetic energy derived from the equipartition theorem (black crosses).

In Fig. 10 it is shown how the system fulfills the equipartition theorem for $T \gtrsim 1.15 T_{\mathrm{BKT}}^{\infty}$, but deviations appear at lower temperatures, where the interaction energy is non-negligible and the approximation in Eq. 12 is not valid.

3 Conclusions

In this work, we have explored the suitability of the Stochastic Projected Gross-Pitaevskii equation (SPGPE) to capture the main features of the Berezinskii-Kosterlitz-Thouless (BKT) transition in a uniform 2D Bose gas. The SPGPE is a modified version of the regular Gross-Pitaevskii equation (GPE) that can capture finite-temperature effects by projecting the wavefunction Ψ onto the coherent region and modeling the thermal fluctuations through a stochastic noise term η, and the dissipation of energy through a damping γ, in accordance with the Fluctuation-Dissipation theorem. The BKT transition, characteristic of two-dimensional systems, is a topological phase transition from a state with only bound vortex-antivortex pairs to one where free vortices proliferate. Through numerical simulations, we have studied several observables of interest that capture the system's behavior across the transition: the quasicondensate fraction n_{qc}, the vortex density n_V, the first order correlation function $g^{(1)}(r)$ and the superfluid fraction f_s.

The results presented are in good agreement with the theoretical predictions of the BKT theory: the unbinding and proliferation of vortices and the suppression of long-range coherence, which destroys superfluidity above the critical temperature $T_{\mathrm{BKT}}^{\infty}$. The critical exponent α extracted from the algebraic fit of $g^{(1)}(r)$ is also accurately reproduced by the simulations.

We also explored the validity of the equipartition theorem for the classical field $\Psi(\vec{r}, t)$. While the energy distribution is consistent with equipartition at high temperatures, deviations emerge as the system enters the low-temperature regime, where the interaction energy is non-negligible.

Overall, our findings confirm the effectiveness of the Stochastic Projected Gross–Pitaevskii equation in capturing the main features of the BKT transition and provide further insight into the interplay between phase coherence, topological excitations, and superfluidity in two-dimensional Bose systems. Future work could extend this approach to more complex systems that could benefit from this classical field formalism. A natural continuation of this study would be to consider a two-component Bose gas, where a second component B, interacting repulsively with the first ($g_{AB} > 0$), is introduced. We expect the vortices of the first component A to seed around the density maxima of the second component B.

Bibliography

[AZBP13] A. J. Allen, E. Zaremba, C. F. Barenghi, and N. P. Proukakis. Observable vortex properties in finite-temperature bose gases. *Phys. Rev. A*, 87:013630, Jan 2013.

[BBD+08] P.B. Blakie†, A.S. Bradley†, M.J. Davis, R.J. Ballagh, and C.W. Gardiner and. Dynamics and statistical mechanics of ultra-cold bose gases using c-field techniques. *Advances in Physics*, 57(5):363–455, 2008.

[Bra24] Ashton S. Bradley. Vortexdistribution.jl. https://github.com/AshtonSBradley/VortexDistributions.jl, 2024.

[CCB+15] Lauriane Chomaz, Laura Corman, Tom Bienaimé, Rémi Desbuquois, Christof Weitenberg, Sylvain Nascimbène, Jérôme Beugnon, and Jean Dalibard. Emergence of coherence via transverse condensation in a uniform quasi-two-dimensional bose gas. *Nature Communications*, 6:6162, 2015.

[CGIA24] Paolo Comaron, Nathan Goldman, Atac Imamoglu, and Ivan Amelio. Quantum impurities in finite-temperature bose gases: Detecting vortex proliferation across the bkt and bec transitions. arXiv preprint, Dec 2024.

[CLDP19] P. Comaron, F. Larcher, F. Dalfovo, and N. P. Proukakis. Quench dynamics of an ultracold two-dimensional bose gas. *Phys. Rev. A*, 100:033618, Sep 2019.

[Dal24] Jean Dalibard. Magnetic interactions between cold atoms: Quantum droplets and supersolid states. Lecture series, Collège de France, March–April 2024.

[GB19] Krzysztof Gawryluk and Mirosław Brewczyk. Signatures of a universal jump in the superfluid density of a two-dimensional bose gas with a finite number of particles. *Phys. Rev. A*, 99:033615, Mar 2019.

[GD03] C. W. Gardiner and M. J. Davis. The stochastic gross–pitaevskii equation: Ii. *Journal of Physics B: Atomic, Molecular and Optical Physics*, 36(23):4731–4753, 2003.

[GRM14] S. Gautam, Arko Roy, and Subroto Mukerjee. Finite-temperature dynamics of vortices in bose-einstein condensates. *Phys. Rev. A*, 89:013612, Jan 2014.

[Gro63] Eugene P. Gross. Hydrodynamics of a superfluid condensate. *Journal of Mathematical Physics*, 4(2):195–207, 02 1963.

[HD11] Zoran Hadzibabic and Jean Dalibard. Two-dimensional bose fluids: An atomic physics perspective. *Rivista del Nuovo Cimento*, 34(6):389–434, 2011.

[KC16] Michikazu Kobayashi and Leticia F. Cugliandolo. Thermal quenches in the stochastic gross-pitaevskii equation: Morphology of the vortex network. *Europhysics Letters*, 115(2):20007, aug 2016.

[KT73] J M Kosterlitz and D J Thouless. Ordering, metastability and phase transitions in two-dimensional systems. *Journal of Physics C: Solid State Physics*, 6(7):1181, apr 1973.

[MW66] N. D. Mermin and H. Wagner. Absence of ferromagnetism or antiferromagnetism in one- or two-dimensional isotropic heisenberg models. *Phys. Rev. Lett.*, 17:1133–1136, Nov 1966.

[Pat96] R. K. Pathria. *Statistical Mechanics*. Butterworth-Heinemann, Oxford, 2 edition, 1996.

[PO56] Oliver Penrose and Lars Onsager. Bose-einstein condensation and liquid helium. *Physical Review*, 104(3):576–584, 1956.

[PRS01] Nikolay Prokof'ev, Oliver Ruebenacker, and Boris Svistunov. Critical point of a weakly interacting two-dimensional bose gas. *Phys. Rev. Lett.*, 87:270402, Dec 2001.

[PRS24] Nick P. Proukakis, Gerasimos Rigopoulos, and Alex Soto. Self-consistent stochastic finite-temperature modelling: Ultracold bose gases with local (s-wave) and long-range (dipolar) interactions. arXiv preprint, Jul 2024.

[PS02] Nikolay Prokof'ev and Boris Svistunov. Two-dimensional weakly interacting bose gas in the fluctuation region. *Phys. Rev. A*, 66:043608, Oct 2002.

[SJCC+19] Raphaël Saint-Jalm, Patricia C. M. Castilho, Édouard Le Cerf, Brice Bakkali-Hassani, Jean-Loup Ville, Sylvain Nascimbène, Jérôme Beugnon, and Jean Dalibard. Dynamical symmetry and breathers in a two-dimensional bose gas. *Physical Review X*, 9(2):021035, 2019.

[VSL+18] J. L. Ville, R. Saint-Jalm, É. LeCerf, M. Aidelsburger, S. Nascimbène, J. Dalibard, and J. Beugnon. Sound propagation in a uniform superfluid two-dimensional bose gas. *Physical Review Letters*, 121(14):145301, 2018.

A Code

A.0.1 First order Euler scheme for the integration of the SPGPE

```
def euler_step_2D(psi):
    # evolves the wavefunction psi (Nx x Ny array) one timestep
    # Scalar variables defined globally:
        # hbar: \hbar
        # g: Coupling constant
        # m: Mass of a single particle
        # Nx, Ny: Number of points in the x,y axis
        # kb: Boltzmann consntant
        # gamma: Dissipation rate
        # T: Temperature
        # k_cut: Maximum momentum included in the projection
        # N_coh: Number of coherent particles
    # Array variables defined globally:
        # Kdos : Kx^2 + Ky^2 (Nx x Ny array)
        # V : External potential (Nx x Ny array)
        # mask : Boolean mask to apply the projector in momentum space

    # FFT of the wavefunction psi
    psi_k = fft.fft2(psi)
    # Laplacian calculated in momentum space
    d2psi_d2 = fft.ifft2(-Kdos * psi_k)
    # Kinetic term of the equation
    H_k = -0.5 * (hbar**2 / m) * d2psi_d2
    # Interaction term of the equation
    H_V= (V+ g*(np.abs(psi)**2))*psi
    # Total effective Hamiltonian of the equation
    H_tot = H_k + H_V
    # Real component of the stochastic noise
    noise_real = rng.normal(loc=0, scale= 1, size= (Nx,Ny))
    # Imaginary component of the stochastic noise
    noise_im = rng.normal(loc=0, scale= 1, size= (Nx, Ny))
    # Noise computed with the correct variance
    noise = np.sqrt((hbar*kb*gamma*T)/(dy*dx*dt))*(noise_real + 1j*noise_im)
    # Timestep
    psi += -(1j*dt/hbar)*(H_tot)*(1 -1j*gamma)
    psi += -(1j*dt/hbar)*noise
    # FFT of the resulting wavefunction to apply the mask (projector onto highly
    ↪  ocuppated modes)
    psi_k_unmasked = fft.fft2(psi)
    k_magnitude = np.sqrt(Kdos)
    mask = k_magnitude <= k_cut
    psi_masked = fft.ifft2(psi_k_unmasked * mask)
    # Normalization to the number og coherent particles
    psi_masked *=
    ↪  np.sqrt(N_coh/np.trapezoid(np.trapezoid(np.abs(psi_masked)**2,y, axis=0),
    ↪  x))
    # Returns the wavefunction evolved and projected
    return psi_masked
```

A.0.2 Routine for the detection of vortices

```python
def detect_vortices(phase_array):
    # Detects vortices calculating the circulation in 2x2 cells
    # Arguments:
        # phase_array: 2D (Nx x Ny) array with the phases of the wavefunction

    # Initializes variables
    rows, cols = phase_array.shape
    vortices = []
    antivortices = []

    # Runs over every 2x2 cell
    for i in range(rows - 1):
        for j in range(cols - 1):
            phi0 = phase_array[i, j]       # top left corner
            phi1 = phase_array[i, j + 1]   # top right corner
            phi2 = phase_array[i + 1, j + 1] # bottom right corner
            phi3 = phase_array[i + 1, j]   # bottom left corner

            # Anti-clockwise circulation
            dphi1 = phi1 - phi0
            dphi2 = phi2 - phi1
            dphi3 = phi3 - phi2
            dphi4 = phi0 - phi3
            total_phase = dphi1 + dphi2 + dphi3 + dphi4

            # Classification vortex/antivortex
            if np.isclose(total_phase, 2 * np.pi, atol=0.1):
                vortices.append((i + 0.5, j + 0.5))
            elif np.isclose(total_phase, -2 * np.pi, atol=0.1):
                antivortices.append((i + 0.5, j + 0.5))
    # Returns:
        # vortices: array of tuples (x,y) with the coordinates of the vortices
        # len(vortices): number of vortices
        # antivortices: array of tuples (x,y) with the coordinates of the
        ↪  antivortices
        # len(antivortices): number of antivortices
    return vortices, len(vortices), antivortices, len(antivortices)
```

A.0.3 Routine computing $g^{(1)}(r)$

```python
def g1_WK(psi_ensemble, nbins):
    # Calculates g1
    # Arguments:
        # psi_ensemble: array of wavefunctions (N x Nx x Ny)
        # nbins : number of bins to dicretize g1(r)
    # Scalar variables defined globally:
        # Rmax : defined as Rmax = R.max()
    # Array variables defined globally:
        # R : array constructed as R = np.sqrt(X^2 + Y^2)

    # Inicialize the array of g1s
    g1_array = []

    # Wiener-Khinchin theorem for each wavefunction of the argument psi_ensemble
    for psi in psi_ensemble:
        psi_fft = np.fft.fft2(psi)
        power_spectrum = np.abs(psi_fft)**2
        corr = np.real(np.fft.ifft2(power_spectrum))
        # Normalization
        g1 = corr / corr[0,0]
        # Shift to ensure g1(0) is at the center of the array
        g1 = np.fft.fftshift(g1)
        g1_array.append(g1)

    # Mean of the arrays
    g1_total = np.mean(g1_array, axis=0)

    # Flatten of radius and g1 arrays
    r_vals = (R / Rmax).flatten() # Radius array normalized to the maximum
    ↪ radius
    g1_vals = g1_total.flatten()

    # Radial bins to group the data
    r_bins = np.linspace(0, np.max(r_vals), nbins + 1)
    r_bin_centers = 0.5 * (r_bins[:-1] + r_bins[1:])
    g1_binned = np.zeros(nbins)
    for i in range(nbins):
        mask = (r_vals >= r_bins[i]) & (r_vals < r_bins[i + 1])
        if np.any(mask):
            g1_binned[i] = np.mean(g1_vals[mask])
        else:
            g1_binned[i] = np.nan

    # Some bins can be empty due to the lack of points in the interval, mask to
    ↪ eliminate NaNs
    mask = np.isfinite(g1_binned)
    r_list = r_bin_centers[mask]
    g1_list = g1_binned[mask]

    # Returns two 1-dimensional arrays with nbins elements each
    return r_list, g1_list
```